Journal of Molecular Liquids 318 (2020) 113894

Contents lists available at ScienceDirect

Journal of Molecular Liquids

journal homepage: www.elsevier.com/locate/molliq

Novel cationic surfactants with cleavable carbamate fragment: Tunable morphological behavior, solubilization of hydrophobic drugs and cellular uptake study

Rushana A. Kushnazarova, Alla B. Mirgorodskaya *, Svetlana S. Lukashenko, Alexandra D. Voloshina, Anastasiia S. Sapunova, Irek R. Nizameev, Marsil K. Kadirov, Lucia Ya. Zakharova

Arbuzov Institute of Organic and Physical Chemistry, FRC Kazan Scientific Center of RAS, 8, ul. Arbuzov, 420088 Kazan, Russian Federation

ARTICLE INFO

Article history:
Received 9 May 2020
Received in revised form 19 July 2020
Accepted 21 July 2020
Available online 25 July 2020

Keywords:
Carbamate-bearing surfactants
Aggregation
Micelle
Vesicle
Solubilization
Cellular uptake

ABSTRACT

The new cationic surfactants containing octyl and dodecyl carbamate moiety in the head group and hexadecyl tail were synthesized and characterized. They demonstrate versatile self-assembling behavior strongly controlled by structural characteristics of amphiphilic molecules. The octyl derivative at a concentration of 0.06 mM forms micelles, which can undergo structural rearrangement with the increase of surfactant content in the solutions (above 0.01 M). Compound with a dodecyl substituent, upon reaching a critical concentration, forms large aggregates without passing through the micellar stage. Combination of different techniques makes it possible to assume that morphological transitions between micelles and vesicles probably occurs with the variation in structural characteristics and concentration of surfactants. This is supported by dynamic light scattering and transmission electron microscopy, as well as changes in characteristics of spectral probes sensitive to micropolarity and packing parameters of aggregates. Aggregates formed showed high solubilization capacity, exceeding that of typical cationic micelles, toward Orange OT hydrophobic dye and poorly water soluble anti-inflammatory drugs, indomethacin and meloxicam. Carbamate-containing surfactants demonstrated the ability to penetrate through cell membrane, delivering the solubilized hydrophobic substances into the cell, which was testified by flow cytometry and fluorescence microscopy with DAPI and Nile Red dyes.

1. Introduction

Cationic surfactants are the most important building blocks used in the creation of supramolecular aggregates, which are widely used in many industries, agriculture, medicine and pharmaceuticals [1–4]. The specifics of their application is related to the fact that hydrophobic effect inducing self-assembly processes in the systems are supplemented by significant electrostatic interactions that determine the structure and properties of the aggregates formed. Thus, the micellar solutions of cationic surfactants used as a medium for a variety of chemical processes have a significant effect on the local concentration and properties of solubilized compounds, which makes it possible to control the rate and mechanism of the reactions [5–7]. The effective adsorption of cationic surfactants on the surface of metal structures and the formation of a protective layer determine their successful application as corrosion inhibitors [8,9]. The presence of a positive charge in combination with amphiphilic matrix ensures the incorporation of cationic surfactants into the lipid bilayers, the effective interaction with intracellular organelles, phosphate residues of nucleic acids and other negatively charged biosubstances, which provides their use for targeted drug delivery and forms the basis for the development of non-viral vectors [10–12]. The directed functionalization of the structure of surfactant molecules by introducing various substituents, in particular, capable of forming hydrogen bonds, allows for involving additional self-assembly mechanisms, changes the aggregation thresholds and the complexation ability, and increases their solubilization effect [13–15].

In recent years, the main trend in molecular design and creation of new cationic surfactants involves the synthesis of compounds that correspond to the principles of green chemistry: the manifestation of high efficiency under mild conditions and low concentration range; low toxicity; the ability to overcome biological barriers. To a large extent, amphiphilic compounds containing cleavable urethane (organic carbamates) residue answer to these criteria. When used as carriers, they meet the requirements of biodegradability and can release the active molecules after overcoming biological barriers, including the blood-brain barrier [16–18]. In addition, carbamate-containing compounds are structural elements of many approved therapeutic agents [19–23], therefore, they can combine the functions of the active substance and the delivery agent of other drugs.

* Corresponding author at: ul.Akad. Arbuzov, Kazan 420088, Russia.
E-mail address: mirgorod@iopc.ru (A.B. Mirgorodskaya).

https://doi.org/10.1016/j.molliq.2020.113894
0167-7322/

Earlier, we obtained and characterized a number of carbamate-containing cationic surfactants, which favorably differ from their trimethylammonium analogues by lower values of critical micelle concentration (CMC), increased solubilization effect, and lower toxicity [24–28]. It was shown that the temperature and concentration thresholds of micelle formation, the surface potential, and the properties of micelles depend not only on the length of the hydrophobic tail at the quaternary nitrogen atom, but also on the length of the alkyl substituent at the nitrogen atom of the carbamate fragment. Smart self-assembling behavior of these amphiphiles encouraged us to synthesize compounds bearing longer chain alkyl substituent in the carbamate group. It was assumed that such modification of the molecular structure can substantially influence packing parameter and lead not only to evolutionary changes in the properties of micellar solutions, but can also cause more significant changes associated with the morphological transition of the system. In the present work, the cationic surfactants containing octyl and dodecyl carbamate moiety in the head group and hexadecyl tail were synthesized and studied. It is known that in some cases surfactants with two hydrocarbon tails can spontaneously associate, forming stable monodisperse vesicles [29–33]. Analogously, natural amphiphilic compounds, i.e. phospholipids bearing two hydrocarbon tails with 16–18 carbon atoms, tend to form vesicle-like aggregates [34,35]. Due to specific geometry factor these compounds are not capable of forming conventional micellar structures in aqueous solutions and form bilayers. In this case, the formation of closed spherical bilayer shells (vesicles) is more favorable both energetically and entropically as compared to infinite flat bilayers [36].

In this regard, the aim of this work was to explore self-assembling behavior of new carbamate-containing surfactants with different length of the hydrocarbon substituent in the head group, to determine aggregation concentration thresholds in aqueous solutions, to examine the structural and solubilization properties of aggregates and to evaluate their potential application as drug delivery systems. To test the above prediction about complicated morphological behavior resulted from appearance of additional long-chain alkyl tail, the data obtained was intended to be compared with those for carbamate-containing surfactants with an ethyl or butyl substituent in the head group [24].

Structural formulas of the studied compounds are presented below:

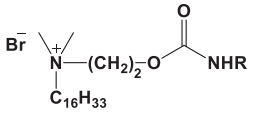

Ur-16(Et) - R = C_2H_5; Ur-16(Bu) - R = *n*-C_4H_9;
Ur-16(Octyl) - R = C_8H_{17}; Ur-16(Dodecyl) - R = $C_{12}H_{25}$

2. Experimental section

2.1. Materials

The studied carbamate-bearing surfactants were prepared by the reaction of hexadecylammonium surfactant containing hydroxyethyl substituent at the head group and alkylisocyanate using diazobicyclooctane as a catalyst as described [24,25]. The structure of the compounds was confirmed by elemental analysis, ESI mass spectrometry, IR- and NMR-spectroscopy data. The obtained characteristics of new carbamate-bearing surfactants with an octyl or dodecyl substituents are given in Supporting information.

Commercially available spectral probes (Orange OT, pyrene, Nile Red (NR), 1,6-diphenylhexatrien-1,3,5 (DPH), 4′,6-diamidin-2-phenylindol dye (DAPI), propidium iodide), drugs (indometacine, meloxicame), alkylisocyanates, diazobicyclooctane (Sigma, 99%) were used without preliminary purification. All solutions were prepared with double-distilled water purified by a Direct-Q 5 UV water purification system; the water resistivity was 18.2 MΩ·cm at 25°C.

2.2. Instruments and methods

Experimental temperatures were maintained at 25 ± 0.1 °C, unless otherwise indicated. All experiments were accurate within ±4%.

Surface tension measurements were performed by the anchor-ring method using KRUSS 6 tensiometer. The cmc values were defined as the concentration corresponding to the breakpoints in the γ vs. logarithm of surfactant concentration plots.

UV–Vis spectra of the spectral probes and drugs solutions were recorded in quartz cells using Specord 250 Plus (Analytik Jena) spectrophotometer equipped with a thermostated cell unit.

The solubilizing capacity of micellar systems toward the probes was determined for their saturated solution as follows. The excess of a crystalline probe was placed in the surfactant solution, stirred vigorously for 1 h and then equilibrated for 48 h (or 24 h for indometacine) at 25 °C. The undissolved probe was filtered, and the filtrate optical density at the maximum absorption was measured.

The mean of micelles size and polydispersity index were determined by dynamic light scattering (DLS) measurement using Malvern ZetaSizer Nano (Malvern Instruments, UK). The source of laser radiation was a He-Ne gas laser with the power of 10 mW and the wavelength of 633 nm. The light scattering angle is 173°. The pulse accumulation time is 5–8 min. The signals were analyzed using a single-plate multichannel correlator coupled with IBM PC compatible computer equipped with the software package for the evaluation of effective hydrodynamic radius of dispersed particles. All samples were analyzed in triplicate, the average error of measurements was approximately 4%.

Transmission electron microscopy (TEM) images were obtained on a Hitachi HT7700 TEM instrument (Japan) operated at 100 kV accelerating voltage. Samples were prepared as follows: a drop of 6 μl was taken from the middle of a freshly prepared solution of a given concentration using a dispenser (Biohit Proline Plus) and applied to a 300 mesh copper grid with a carbon-formvar support film (Agar Scientific). A drop completely covers the grid. The sample preparation process is carried out at room temperature. Next, the sample is dried in a muffle furnace at a temperature of 30 °C.

Fluorescent spectra were recorded using Varian Cary Eclipse spectrophotometer. Emission spectra were recorded within the interval of 350–500 nm for pyrene and 500–800 nm for Nile Red at a scanning rate of 120 nm/min using a 1.0 cm path length cuvette; the excitation of the sample was occurred at a wavelength of 335 nm pyrene and 480 nm Nile Red.

Steady-state fluorescence anisotropy of DPH was measured on Varian Cary Eclipse spectrometer equipped with filter polarizers. The concentration of fluorescence probe DPH in all measurements was equal to 0.18 mM. A quartz cell of 1 cm path length was used for all fluorescence measurements. DPH were excited at 361 nm, and the fluorescence intensity was measured at 450 nm. The excitation and emission slit widths were 2.5 and 5 nm, respectively. Calculation of the anisotropy parameter (r) is based on the relationship $r = (I_v - I_h)/(I_v + 2I_h)$, where I_v and I_h are the intensities of fluorescence of the vertically and horizontally polarized emission, respectively, under excitation of samples by the vertically polarized light [37]. The embedded software automatically determined the correction factor and anisotropy value.

2.3. Cytotoxicity assay

Cytotoxic effects of the test compounds on normal and cancer cells were estimated by means of the multifunctional Cytell Cell Imaging system (GE Health Care Life Science, Sweden) using the Cell Viability Bio App which precisely counts the number of cells and evaluates their viability from fluorescence intensity data. Two fluorescent dyes that selectively penetrate the cell membranes and fluoresce at different wavelengths were used in the experiments. A low-molecular-weight 4′,6-diamidin-2-phenylindol dye is able to penetrate intact membranes of living cells and color nuclei in blue. High-molecular propidium iodide dye penetrates

only dead cells with damaged membranes, staining them in yellow. As a result, living cells are painted in blue and dead cells are painted in yellow. The M-Hela clone 11 human, epithelioid cervical carcinoma, strain of Hela, clone of M–Hela; WI-38 VA-13 cell culture, subline 2RA (human embryonic lung) from the Type Culture Collection of the Institute of Cytology (Russian Academy of Sciences) and Chang liver cell line (Human liver cells) from N. F. Gamaleya Research Center of Epidemiology and Microbiology were used in the experiments. The cells were cultured in a standard Eagle's nutrient medium manufactured at the Chumakov Institute of Poliomyelitis and Virus Encephalitis (PanEco company) and supplemented with 10% fetal calf serum and 1% nonessential amino acids. The cells were plated into a 96-well plate (Eppendorf) at a concentration of 1×10^5 cells/ml, 150 μl of medium per well, and cultured in a CO_2 incubator at 37 °C. Twenty four hours after seeding the cells into wells, the compound under study was added at a preset dilution, 150 μl to each well. The dilutions of the compounds were prepared immediately in nutrient media. The experiments were repeated three times. Intact cells cultured in parallel with experimental cells were used as a control [38].

2.4. Flow cytometry

Chang liver cells in an amount of 1×10^5 cells/well in a final volume of 2 ml were seeded in 6-well plates (Eppendorf). After 24 h of incubation, free NR, NR in solutions of Ur-16 (Octyl) or Ur-16 (Dodecyl) at a concentration of 60 μM was added to the wells and cultured for 24 h in a CO_2 incubator. Cellular absorption was analyzed by flow cytometry (Guava easy Cyte 8HT, USA). Flow cytometry was used to generate statistics on the uptake of surfactant based systems by Chang liver cells. Free NR was used as a fluorescent probe (red fluorescence). Untreated cells were used as a negative control.

2.5. Fluorescence microscopy

Chang liver cells in an amount of 1×10^5 cells/well in a final volume of 2 ml were seeded in 6-well plates with coverslips at the bottom of each well. After 24 h of incubation, free NR and NR in a solution of the surfactant at the concentration of 60 μM were added to the wells and cultured for 24 h in a CO_2 incubator. Then, after treatment with free NR and NR in solution of Ur-16 (Octyl) or Ur-16 (Dodecyl), Chang cells were fixed and stained with DAPI (blue). Studies were performed using a Nikon Eclipse Ci-S fluorescence microscope (Nikon, Japan) at a magnification of 1000×.

The cytometric results were analyzed by the Cytell Cell Imaging multifunctional system using the Cell Viability BioApp application. The data in the tables and figures are given as the mean ± standard error.

3. Results and discussion

To assess the aggregation behavior of new carbamate-containing surfactants, Ur-16(Octyl) and Ur-16(Dodecyl) a number of complementary physicochemical methods was used.

3.1. Tensiometry

Tensiometry is one of the most important methods traditionally used in colloid chemistry to characterize the behavior of surfactants in solutions. The obtained surface tension isotherms make it possible, first of all, to determine the concentration region of micellization of the studied compounds. The breakpoint in the surface tension dependence on lgC_{surf} corresponds to the critical micelle concentration, and for Ur-16(Octyl) this value is $5{\cdot}10^{-5}$ M (Fig. S1), which is significantly lower than for comparison compounds, having an ethyl or butyl substituent in the carbamate moiety. Unusual behavior was observed in the case of Ur-16(Dodecyl), for which we fail to determine the CMC by the tensiometry method. Within the whole concentration range from $1{\cdot}10^{-7}$ M to $1{\cdot}10^{-3}$ M no decrease in surface tension occurred (Fig. S1). Such kind of behavior is typical for two-tailed surfactants, for which the tensiometry method appeared to be unsuitable to determine the aggregation threshold. In analogy with literature data [39,40] it can be assumed that the aggregation of Ur-16(Dodecyl) in the bulk of the solution occurs before its molecular monolayer forms at the water-air interface. As summarized in [40] two-tailed surfactants tend to form spontaneously the vesicle-like aggregates, with the aggregation threshold occurring at ≤0.01 mM. To test this assumption further examination of the samples was carried out, with alternative techniques involved.

3.2. Dynamic light scattering data

The elucidation of the morphology of aggregates is generally a challenging problem due to the following facts (1) even in the case of methods providing the direct visualization of particles their results need delicate interpretation, with the conditions of experiments taken into account; (2) the majority of methods are indirect and may involve the use of probes, which can affect the results; (3) combination of different techniques can probably give the correct results providing that they were treated with care. Based on this consideration, a variety of techniques were involved in our study to examine the size and morphological behavior of the systems, with the DLS method giving the primary information.

Fig. 1 shows the size distribution of aggregates, taking into account the signal intensity of all particles in the solutions. In the case of Ur-16 (Octyl), the micelle-like aggregates with a hydrodynamic diameter of 5–10 nm are formed near the CMC. With the increase of surfactant concentration of more than 0.08 mM large aggregates are formed with a hydrodynamic diameter (D_h) of 50–80 nm (Figs. 1a, S2). The increase in the size of aggregates can be caused by either the rearrangement of spherical micelles into cylindrical ones or the formation of aggregates of vesicular structures. For Ur-16(Dodecyl) over a wide range of concentrations, the size of particles remained practically unchanged and amounted to 80–110 nm (Fig. 1b), with the polydispersity index lying in the range 0.2 to 0.3. The size of aggregates, as well as its independence from the concentration of surfactants can be characteristic signs of the formation of vesicles in solutions (with respect to concentration dependent phase transformation) [41].

High stability of the Ur-16(Dodecyl) aggregates in aqueous solutions should be noted, their sizes remained constant during the month (Fig. S3), which testified the formation of vesicle-like aggregates as well.

3.3. Transmission electron microscopy data

To obtain additional information, aggregates of carbamate-bearing surfactants in solutions were visualized using transmission electron microscopy technique (Figs. 2, S4). The figures show that Ur-16(Octyl) self-assemble in aggregates with a uniform density distribution. Their diameter is 12–18 nm at a concentration of 0.05 mM, and 45–55 nm at a concentration of 0.1 mM (Fig. 2a), which is in accordance with DLS data. For Ur-16(Dodecyl), TEM detects large particles of different types, including those of roughly spherical or elongated shape and aggregates with inhomogeneous density, consisting of a denser elongated core surrounded with a loose mantle (Figs. 2, S4). The former exist at concentration of ≥1 mM, while the latter are probably their precursors occurring at lower concentrations. It can be assumed that a longer and conformationally flexible substituent in the head group of a carbamate-containing surfactant complicates the formation of dense homogeneous aggregates in the condition of deficit of amphiphilic molecules available. It is difficult to compare directly DLS data with TEM images, due to the sphere approximation used in the DLS formalism, and hydrate shell size contributing to the particle diameter. Besides, sample preparation assumes evaporation of the solvent, which can affect TEM result. Nevertheless, the formation of large aggregates was postulated by both techniques, with the vesicle occurrence assumed. For both surfactants, an increase in the surfactant concentration probably leads to particle coalescence and the appearance

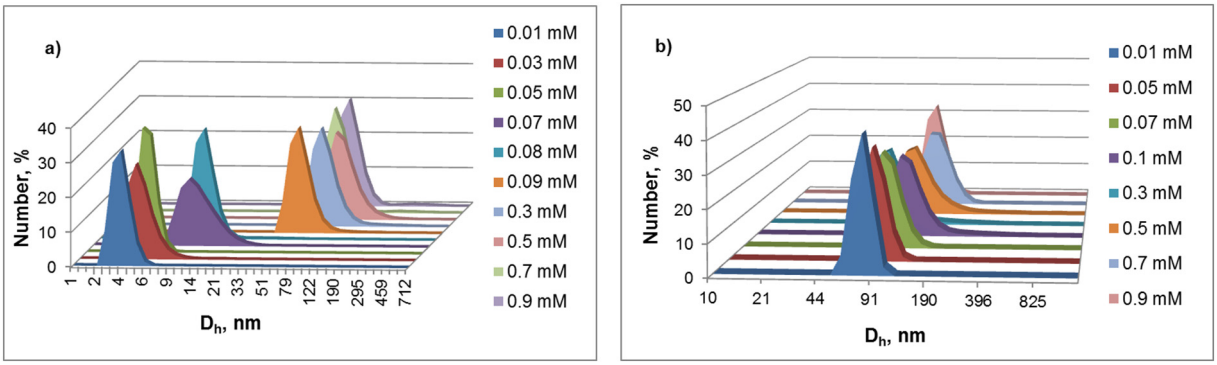

Fig. 1. Particle size distribution by number in micellar solutions of carbamate-containing surfactants: a - Ur-16(Octyl); b - Ur-16(Dodecyl).

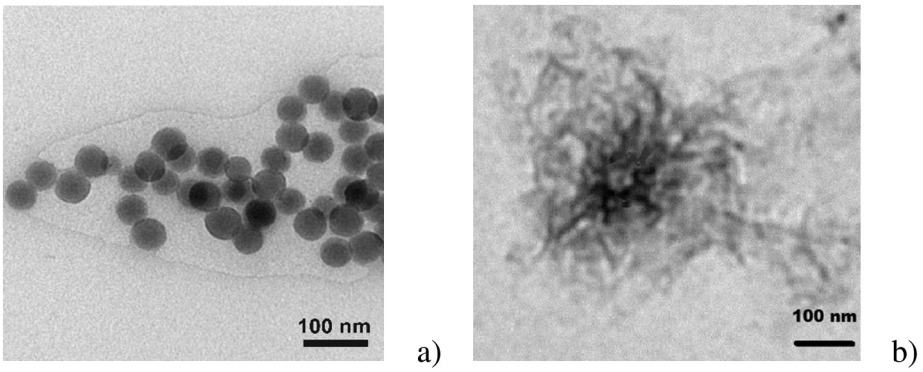

Fig. 2. Transmission electron microscopy image for Ur-16(Octyl) (a) and Ur-16(Dodecyl) (b);

of large aggregates with a diameter reaching about 1 μm, in which the subtle structural features are not manifested (Figs. S4b, S4c).

C = 0.1 mM, 25 °C.

3.4. Investigation of the aggregation behavior of carbamate-containing surfactants using spectral probes

To further elucidate aggregation behavior of carbamate-containing surfactants, different techniques involving spectral probes were used. It is known that the aggregation of surfactants in solution underlies their ability to solubilize the low-polar compounds, which leads to an increase in their solubility due to localization in hydrophobic domains of organized systems, in particular, a non-polar micelle core or vesicle bilayer.

The solubilizing effect of the system is determined by the chemical structure of the surfactant and varies depending on the charge of the head group, the size of the hydrophobic domain, the ability to realize specific interactions, and the properties of the solubilizate. The structural formulas of hydrophobic probes used in this work are given below.

3.4.1. Solubilization of hydrophobic probe Orange OT

To confirm the formation of aggregates in solutions of Ur-16(Octyl) and Ur-16(Dodecyl), their solubilization effect on the low-polar dye Orange OT was studied. This dye, characterized by the presence of an intense absorption band at 495 nm, is widely used as a highly sensitive probe for the quantitative assessment of the solubilization capacity of surfactant-based systems [15]. The extensive database for this dye makes it possible to compare the studied surfactants with the similar compounds.

Considering the fact that Orange OT is practically insoluble in water, a sharp increase in the optical density of solutions related with the process of its solubilization in surfactant aggregates allows us to determine the concentration threshold of aggregation (Figs. 3, S5, S6a,b). Noteworthy, despite the fact that no decrease in surface tension occurred in the case of dodecyl derivatives preventing the measurement of the aggregation threshold, reliable evidence of aggregate formation for Ur-16(Dodecyl) is provided by the dye solubilization technique. For both compounds, the obtained values of critical concentration of aggregation (CMC or critical vesicle concentration) are lower than for analogues with a shorter substituent in the carbamate fragment (Table 1), while

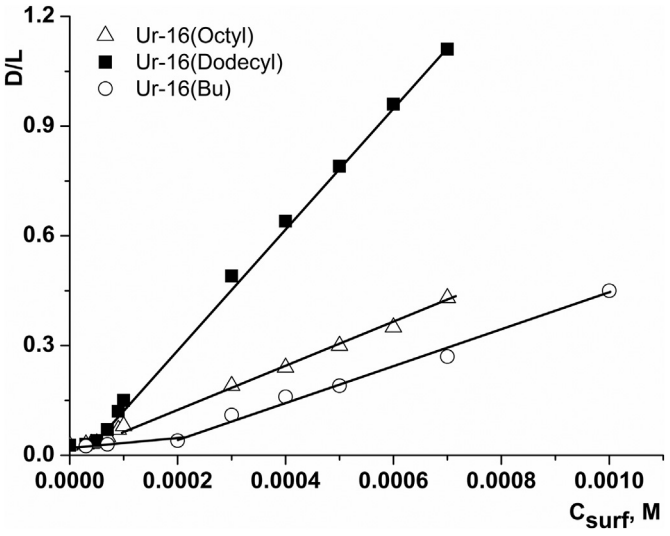

Fig. 3. Dependence of optical density of saturated Orange OT solutions at a wavelength of 495 nm on the concentration of surfactants.

Table 1
The critical concentration of aggregation (CAC) of carbamate-containing surfactants determined by various methods; solubilization capacity with respect to Orange OT.

	Surfactants	CAC, mM			$S_{Orange\ OT}$, mole dye/mol surfactant
		Tensiometry	Orange OT solubilization	Pyrene solubilization	
1	Ur-16(Et)	0.70 [24]	0.75 [24]	0.80	0.024 [24]
2	Ur-16(Bu)	0.24 [24]	0.21 [24]	0.30	0.027 [24]
3	Ur-16(Octyl)	0.049	0.057	0.06	0.030
4	Ur-16(Dodecyl)		0.04	0.045	0.088

the value for Ur-16(Octyl) coincides with the CMC determined by tensiometry (Table 1).

The absorbance versus concentration plot provide the basis for the determination of the solubilizing capacity (S) of the micellar system: $S = b/\varepsilon$, where b is the slope of the linear part of the dependence and ε is the molecular extinction coefficient of Orange OT equal to 18,720 $l \cdot mol^{-1} \cdot cm^{-1}$. From the results obtained (Table 1), it follows that the solubilization capacity of all carbamate-containing surfactants studied is higher than that of CTAB (S = 0.015 [15]).

Apparently, the presence of a fragment capable of hydrogen bonding makes it possible to use the additional interaction mechanisms between the dye and the micelle, which facilitates the processes of solubilization. The value of S increases in the series Ur-16(Et) < Ur-16(Bu) < Ur-16 (Octyl) < Ur-16(Dodecyl). Noteworthy, the fact that solubilization capacity of Ur-16(Dodecyl) is significantly higher compared to other analogues allows us to suggests that aggregates of different morphology are formed in this case, with a large hydrophobic domain capable of binding nonpolar Orange OT, which is in line with the assumption on vesicles existence.

3.4.2. Fluorescence spectroscopy measurements

Fluorescence spectroscopy using various molecular probes is a powerful method for studying the aggregation behavior of surfactants, including microenvironmental properties, morphological characteristics and assessing the CAC of surfactants in aqueous solutions. In this work, pyrene, DPH, and NR were used as sensitive fluorescent probes, with pyrene the most widely used [37,42,43]. The position of the emission maxima in the spectra of this compound slightly depends on the solvent, while their intensity responds to changes in the properties of the medium and, above all, to the polarity of the microenvironment. The fluorescence spectra of pyrene were recorded at different concentrations of carbamate-bearing surfactants in solutions. The typical spectra are shown in Fig. S.7. The intensity ratio of the first 373 nm (I_1) and third 384 nm (I_3) vibronic emission bands of pyrene can be used to estimate the influence of the medium [42], which is sensitive to micropolarity in the probe localization zone and, as a rule, decreases with increasing surfactant concentration, because of the decrease in polarity of the microenvironment. Based on the experimental data of pyrene emission spectra in surfactant solutions, the dependences of the ratio (I_1/I_3) on the surfactant content were plotted (Fig. 4). The obtained dependences are characterized by two sections with different slopes, the intersection point corresponds to the CMC. The CMC values obtained by the fluorescence method are in good agreement with the other methods and are 0.06 mM and 0.045 mM for Ur-16(Octyl) and Ur-16(Dodecyl), respectively (Table 1). Based on the values of I_1/I_3, the polarity of the head group of surfactants and the localization of pyrene in micelles can be determined. For pyrene dissolved in water, the value of I_1/I_3 is 1.6. The ratio $I_1/I_3 < 0.6$ indicates the location of the probe in the hydrocarbon core of the micelle. The location of pyrene in the surface layer of micelles is characterized by a ratio in the range 1.0–1.4 [37]. The parameter characterizing the changes in micropolarity decreases in the series Ur-16(Et) < Ur-16(Bu) < Ur-16(Octyl) < Ur-16 (Dodecyl) and varies from 1.1 to 0.85 (Fig. 4). This testifies that, as the length of the alkyl substituent in the carbamate fragment increases,

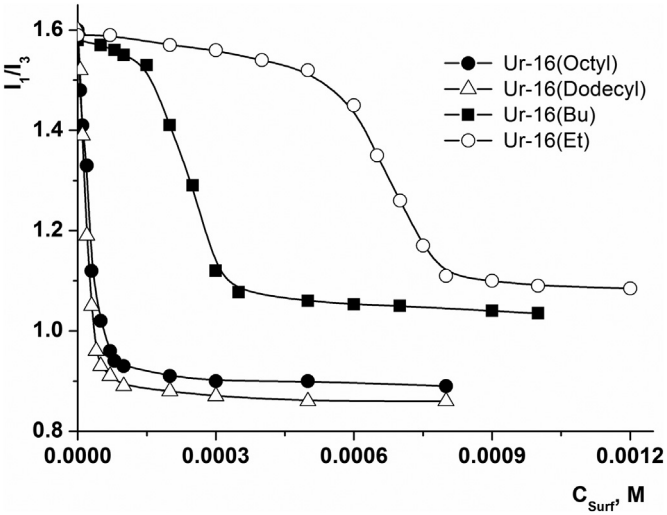

Fig. 4. Dependences of the ratio (I_1/I_3) in fluorescence emission spectra of pyrene on the content of carbamate-containing surfactants.

the localization of the probe moves from the surface layer into the depth of the hydrophobic region. Therefore, the structural factor may serve as a key tool for tailoring the microenvironmental characteristics of aggregates, thereby varying the localization and physicochemical behavior of the guest molecules.

However, the use of pyrene does not provide the information about the structure of aggregates that fluorescent probes with twisted intramolecular charge transfer (TICT) are capable of giving. These compounds represent a class of fluorophores whose properties exponentially depend on the local polarity of the medium. The photoinduced full transfer of intramolecular charge results in the molecule twisting into two mutually perpendicular parts. The produced TICT excited state has much higher dipole moment than the ground state and is thus very sensitive to the change of microenvironment. Nile Red is typical TICT probe [44–51].

3.4.3. Micropolarity study with the use of fluorescent dye Nile Red

NR is one of the most well-known highly fluorescent dyes displaying remarkable solvatofluorochromism. Its fluorescence depends on the polarity of the medium, and its increase leads to a significant bathochromic shift of the absorption and emission maxima. This is due to the large dipole moment of the molecules in the excited state and the existence of TICT, which occurs easier in polar media than in nonpolar ones [43–48]. The main emission band, characteristic for NR aqueous solutions, corresponds to 660 nm, however, it can slightly change its position in other media.

Thus, the NR fluorescence spectra recorded in solutions of Ur-16(Et) (Fig. 5a) and Ur-16(Dodecyl) (Fig. 5b) with a wide range of surfactant concentrations are characterized by an emission band with a maximum at 627 nm. The observed hypochromic shift by 30 nm with respect to the NR fluorescence spectra in water can be explained by the fact that the probe penetrates the palisade layer of the aggregates, while the polarity of its microenvironment decreases, whereas the increase in signal intensity reflects an increase in the solubility of the probe in the system.

NR fluorescence spectra in Ur-16(Dodecyl) solutions at low surfactant concentrations also have only one emission band with a maximum at 627 nm (Fig. 5b). However, a second peak appears at 569 nm above the CAC of this compound in the short-wavelength region of the NR spectra, which is related with the emission of the dye preferentially the in-plane local environment (LE). The intensity of this band increases with increasing of Ur-16(Dodecyl) content. According to [47,48], NR molecules driven out from the palisade layer of aggregates to the hydrophobic region with the increase of surfactant concentration leading to their separation from water molecules, which penetrate only into the

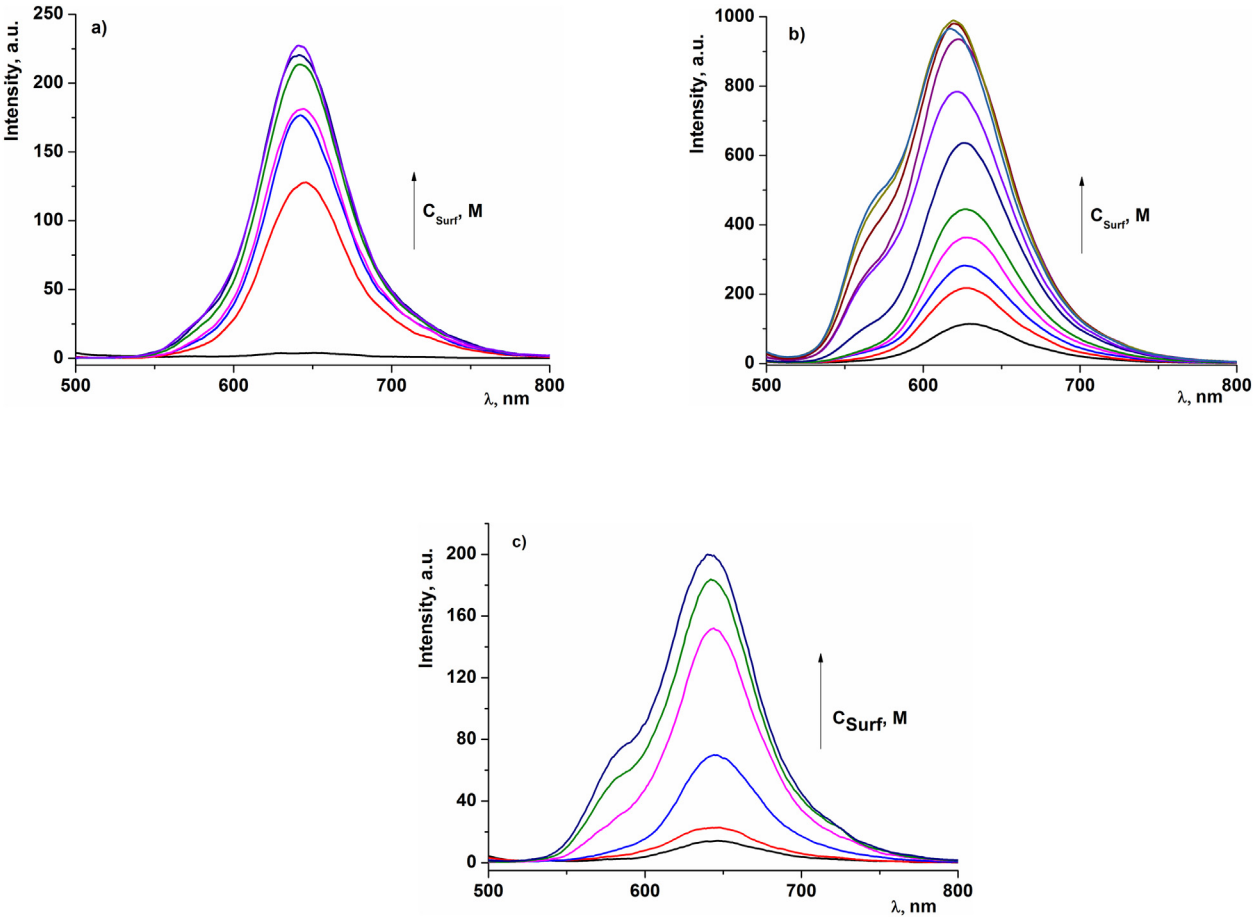

Fig. 5. NR fluorescence spectra in solutions of Ur-16(Dodecyl) (a), Ur-16(Et) (b) and Ur-16(Octyl) (c) on surfactant concentration, 25°C.

surface layers. In this case, the hydrogen bonds between water and NR are destroyed, and this is an unfavorable factor for the TICT state formation. This is especially pronounced in the case when vesicles with a bulky hydrophobic domain are formed in surfactant solutions. In the spectra of NR solutions in Ur-16(Octyl) in addition to the peak at 630 nm, another second peak appeared at 570 nm (Fig. 5c), however, its intensity is much lower than in systems with Ur-16(Dodecyl) and is manifested at concentrations significantly higher than CMC. A measure that estimates the contribution of the TICT and LE states is the ratio of the intensity of long-wave and short-wave radiation (I_a and I_b, respectively), which is usually used in the analysis of NR incorporation into vesicles. Fig. 6 shows the dependence of I_a/I_b on the concentration of carbamate-containing surfactants. For Ur-16(Dodecyl), a monotonic decrease of I_a/I_b is observed, which indicates a gradual inclusion in the core, which is in agreement with the formation of vesicles in all studied concentration range. The similar behavior was observed for Ur-16 (Octyl), however, only at a concentration higher than 0.1 mM, where a significant increase in the size of the resulting aggregates was detected by DLS.

3.4.4. Fluorescence anisotropy of 1,6-diphenylhexatrien-1,3,5

An informative method for determining the morphology of aggregates is the measurement of the anisotropy (r) of DPH-type probes using fluorescence spectroscopy [50]. DPH is a well-known membrane fluidity probe that can easily be placed in the hydrophobic region of a vesicle due to its rigid rod-like structure. The higher the restriction of DPH motion in the hydrophobic domain, the greater the value of anisotropy. In general, DPH always exhibits greater fluorescence anisotropy compared to micellar aggregates. Higher r values correspond to a more ordered state, while lower r values correspond to a loose packing of monomers. Therefore, the r parameter is very sensitive to the transition from micelle to vesicle and vice versa. As a rule, the r value close to 0.2 indicates the presence of a bilayer structure characterized by compact packing of amphiphilic molecules, while $r < 0.1$ allows us to predict micelle-like aggregates, which provide the higher lability for the probe [51].

Fig. 7 shows the concentration dependence of anisotropy for the studied surfactants. The r value increased from 0.05 to 0.18 for Ur-16(Octyl), while in the case of Ur-16(Dodecyl) it remained roughly constant around

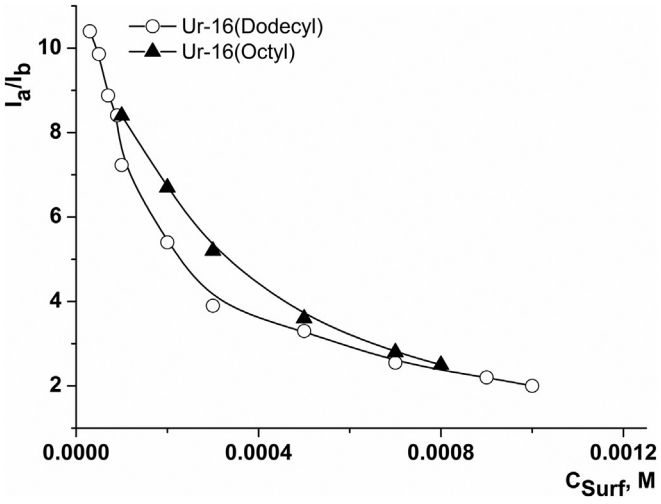

Fig. 6. Dependence of I_a/I_b on the concentration of carbamate-containing surfactant.

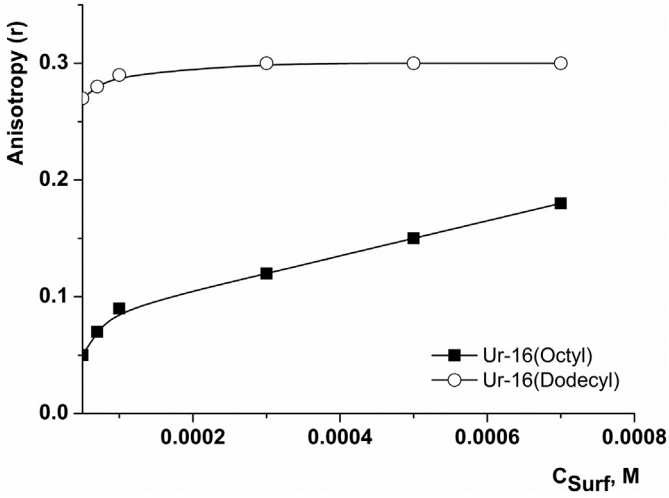

Fig. 7.. Dependence of fluorescence anisotropy r of fluorescence probe DPH on surfactant concentration; 25°C.

the value of 0.3. The dependence is in good agreement with the data obtained by dynamic light scattering. It is significant that anisotropy of fluorescence changes with the concentration of Ur-16(Octyl), which is in line with the structural transition assumed. At the same time little or zero changes in packing mode are assumed in the case of Ur-16(Dodecyl) with an increase in concentration (enlarging in the size in TEM images is probably due to the agglomeration of aggregates upon sample preparation). This is in consistence with the roughly constant value of the anisotropy in Fig. 7.

Thus, this method also suggests that Ur-16(Dodecyl) does not form micelles in aqueous solutions. Probably, its aggregation in solution leads to the formation of vesicles immediately. Meanwhile, Ur-16 (Octyl) firstly form micelles, which can be transformed into vesicles with an increase in surfactant concentration.

To sum up, the combination of several techniques allows us to elucidate morphological behavior of novel carbamate-bearing surfactants. Relatively simple case is observed for Ur-16(Octyl) systems at low concentrations, when hydrodynamic diameter of aggregates does not exceed 10–20 nm. This can be reliably attributed to the existence of spherical or slightly elongated micelles. Other cases, especially morphological behavior of Ur-16(Dodecyl) systems took additional investigations and assumptions. Nevertheless, careful analysis of results of DLS, TEM and a number of dye solubilization and fluorescence probe techniques, especially the fluorescence anisotropy assay makes it possible to conclude that different morphologies are realized for Ur-16 derivatives depending on the structure and concentration of surfactants. In particular, high probability occurs that vesicle-like aggregates are formed in Ur-16(Dodecyl) systems, while micelle-to-vesicle transition can occur in Ur-16(Octyl) solutions.

3.5. Increase of drug solubility

The high solubilization capacity of the systems based on carbamate-containing surfactants with respect to spectral probes initiated their use as nanocontainers to increase the solubility and bioavailability of drugs. The investigation was carried out using non-steroidal anti-inflammatory drugs indomethacin and meloxicam, which were also studied earlier [52–55]. Under these conditions, the indomethacin content can be determined by the absorption maximum at 320 nm (ε 5800 $mol^{-1}l\ cm^{-1}$) [54], and for meloxicam at 366 nm (ε 14,700 $mol^{-1}l\ cm^{-1}$) [27]. Fig. 8 shows the results reflecting a decrease in the optical density of indomethacin and meloxicam in micellar systems formed on the basis of carbamate-containing surfactants studied in this work. The solubilization capacity of the studied systems was calculated based on them. (Table 2).

The data obtained indicate that the value of solubilization capacity increases and reaches the maximum for Ur-16(Dodecyl) with the increase of alkyl substituent length in the carbamate fragment. Adding this compound to water at a concentration of 0.5 mM can increase the solubility of indomethacin by 14 times, and meloxicam by 30 times. Such growth of the solubility of drugs will increase their bioavailability and reduce the dose of the drug, thereby decreasing the negative effect.

3.6. Biological study

An important factor determining the therapeutic effect of the dosage form is not only the concentration of the active base, but also the ability of the whole formulation to overcome cellular barriers. Systems based on cationic surfactants in some cases can exhibit such properties [56,57].

The ability of the studied carbamate-containing surfactants to penetrate into the cell was visualized using fluorescence microscopy on a human Chang liver cell line. The chosen concentration of surfactants was close to the value of their CMC and did not exceed the IC_{50} values found from the cytotoxicity experiments (Table S1). The data obtained are presented in Fig. 9.

To label the nucleus of the cell, a DNA intercalating dye DAPI (blue spot) was used, the luminosity of which does not depend on the presence of surfactants in solutions. In the absence of a surfactant, NR enters the cell in small quantities, as evidenced by its weak red fluorescence.

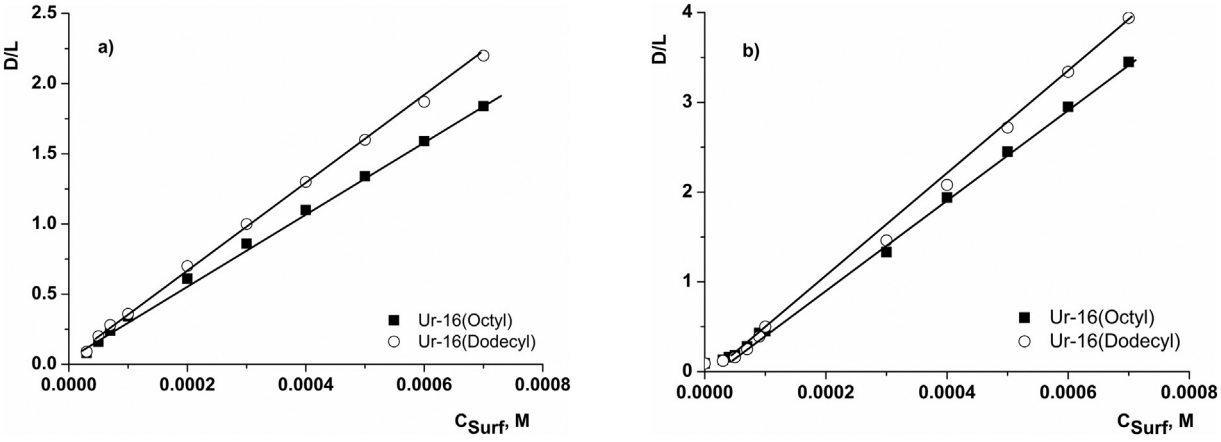

Fig. 8. Dependences of optical density of saturated solutions with indomethacin (a) and meloxicam (b) at a wavelength of 320 nm and 366 nm, respectively, on the concentration of surfactants, pH 4.4, 25°C.

Table 2
Solubilization capacity of surfactants toward Indomethacin, Meloxicam.

	Surfactant	S, mole dye/mol surfactant	
		Indomethacin	Meloxicam
1	Ur-16(Et)	0.25	0.19
2	Ur-16(Bu)	0.38	0.23
3	Ur-16(Octyl)	0.44	0.35
4	Ur-16(Dodecyl)	0.53	0.36

The presence of carbamate surfactants leads to a sharp increase in signal intensity. This suggests that the studied surfactant-based systems are capable to overcome the cell barriers and facilitate the delivery of solubilized NR to the cell. The penetration of this probe into cells was confirmed by the presence of purple fluorescent spots on fused images of DAPI and NR in the presence of surfactants. The luminous intensity increases from Ur-16(Octyl) to Ur-16(Dodecyl), which indicates the better transport properties of the latter. The same conclusion can be drawn by considering the results of flow cytometry using Chang liver cells for NR probe in the above-mentioned systems (Fig. 10).

The fluorescence intensity of NR in carbamate-bearing surfactant solutions is higher than that of the free probe, and it increases from Ur-16 (Octyl) to Ur-16(Dodecyl). The novel surfactants under study provided more effective penetration of NR to a living cell than CTAB (Fig. 10) which is considered to be a reference cationic surfactant often used for comparison. At the same time essential limitation of CTAB systems is high toxicity preventing their wide practical application. This suggests that carbamate surfactants act as carriers that facilitate the delivery of a hydrophobic dye to a cell, which opens up prospects for their use as delivery systems of therapeutic agents widely used in medicine.

4. Conclusions

Thus, new cationic surfactants containing octyl and dodecyl carbamate moiety in the head group and hydrophobic hexadecyl tail significantly differ from their ethyl- or butyl-substituted analogues by their behavior in solutions and solubilizing action. They are capable of aggregation at significantly lower concentrations, herein Ur-16(Dodecyl) at a concentration of 0.04 mM already exists in the form of vesicles, while Ur-16(Octyl) at a concentration of 0.06 mM forms micelles, which are transformed into vesicles with an increase in the surfactant content. Importantly, these findings can be used to trigger the cascade 'molecular structure/concentration variation – morphological transitions – microenvironmental changes – functional activity modification'. The resulting

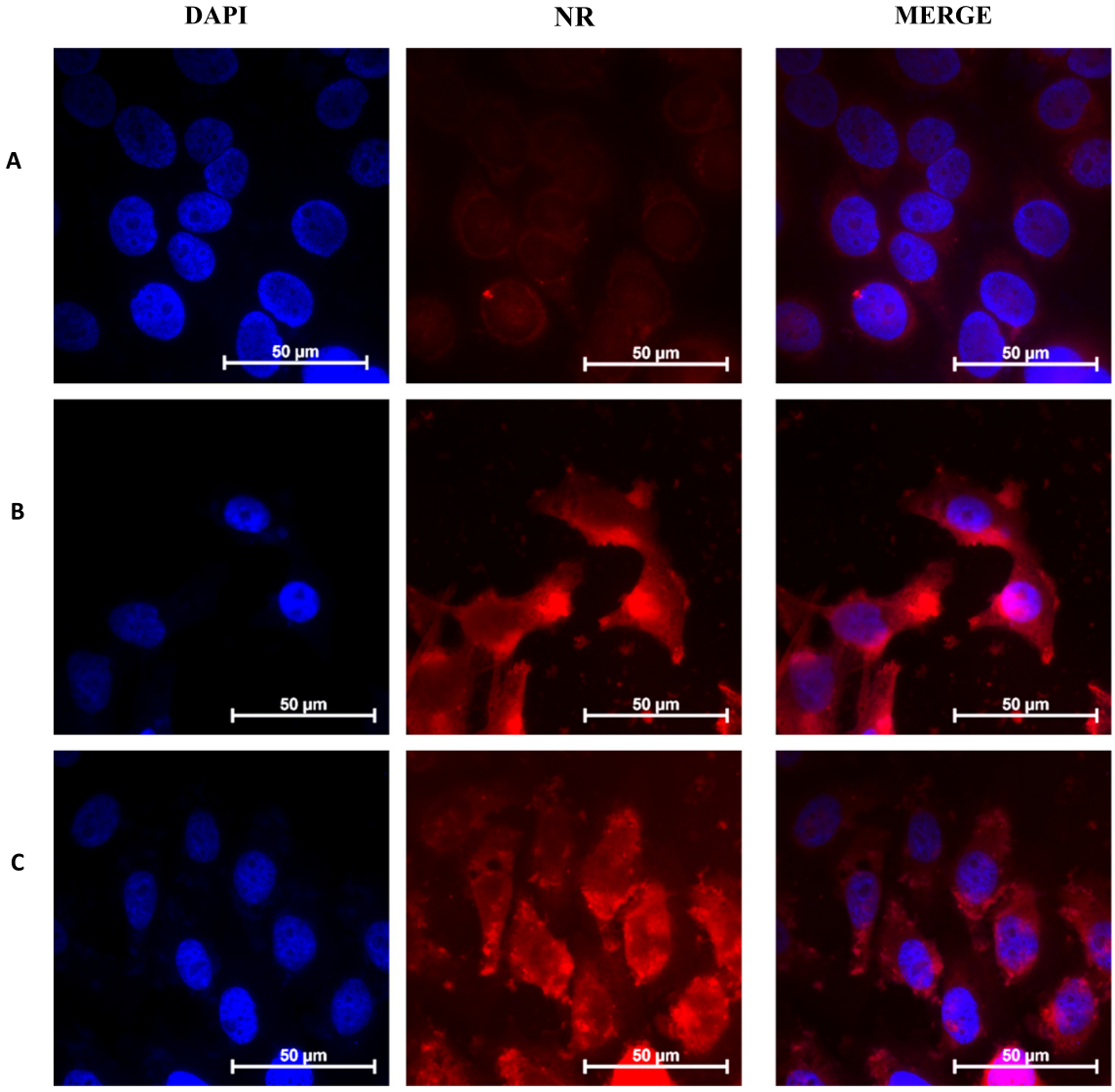

Fig. 9. Cell uptake of free and formulated spectral probes (DAPI and NR) by Chang liver cells using the method of fluorescence microscopy. A - without surfactants, B - Ur-16(Octyl), 60 μM, C - Ur-16(Dodecyl), 60 μM.

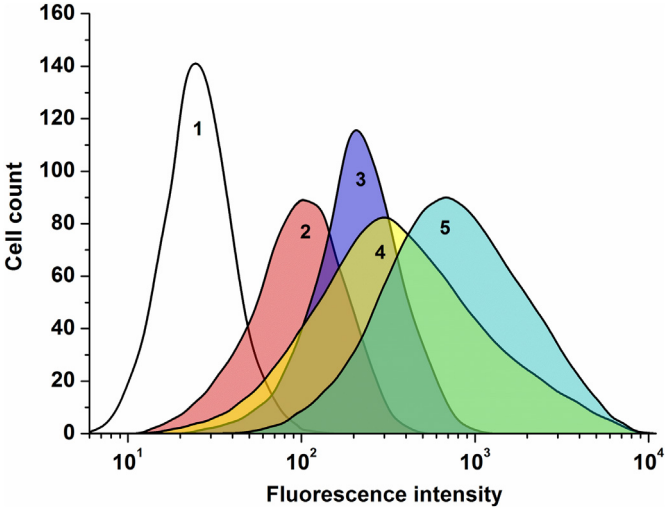

Fig. 10. Cellular uptake study of supramolecular systems based on new carbamate-bearing surfactants; 1 – Control, 2 - Nile Red (free); 3 - Nile Red in solution of CTAB – 10 μM; 4 - Nile Red in solution of Ur-16(Octyl) – 60 μM; 5 - Nile Red in solution of Ur-16 (Dodecyl) – 60 μM (Chang liver, $C_{NR} = 0.5$ μM). (For interpretation of the references to color in this figure legend, the reader is referred to the web version of this article.)

vesicles are characterized by a high solubilization capacity with respect to hydrophobic compounds, in particular, Orange OT dye and anti-inflammatory drugs, indomethacin and meloxicam. It was shown that they exhibit high efficiency even at low concentrations of added surfactants. Thus, the presence of Ur-16(Dodecyl) at a concentration of 0.5 mM can increase the solubility of indomethacin by 14 times, and meloxicam by 30 times. A growth in the solubility of drugs will increase their bioavailability and reduce therapeutic doses of the drug, thereby decreasing the negative side effect. It was demonstrated the ability of the carbamate-containing surfactants studied to overcome cell barriers and ensure the delivery of solubilized substances into a living cell. These data allow us to recommend the systems studied as effective nanocontainers with tunable morphological behavior and superior biomedical potential.

CRediT authorship contribution statement

Rushana A. Kushnazarova: Methodology, Investigation, Writing - original draft. **Alla B. Mirgorodskaya:** Data curation, Supervision, Writing - review & editing. **Svetlana S. Lukashenko:** Investigation. **Alexandra D. Voloshina:** Methodology, Investigation. **Anastasiia S. Sapunova:** Methodology, Investigation. **Irek R. Nizameev:** Visualization. **Marsil K. Kadirov:** Visualization. **Lucia Ya. Zakharova:** Conceptualization, Funding acquisition, Writing - review & editing.

Declaration of competing interest

The authors declare that they have no known competing financial interests or personal relationships that could have appeared to influence the work reported in this paper.

Acknowledgements

This work is supported by the Russian Science Foundation (grant № 19-73-30012).

Appendix A. Supplementary data

Supplementary data to this article can be found online at https://doi.org/10.1016/j.molliq.2020.113894.

References

[1] S. Le Guenic, L. Chaveriat, V. Lequart, N. Joly, P. Martin, Renewable surfactants for biochemical applications and nanotechnology, J. Surfactant Deterg. 22 (1) (2019) 5–21, https://doi.org/10.1002/jsde.12216.
[2] L. Sanders, Cationic Surfactants: Properties, Uses and Toxicity, Nova Science Publishers Inc, UK, 2016.
[3] P. Sar, A. Ghosh, A. Scarso, B. Saha, Surfactant for better tomorrow: applied aspect of surfactant aggregates from laboratory to industry, Res.Chem.Intermed. 45 (2019) 6021–6041, https://doi.org/10.1007/s11164-019-04017-6.
[4] S.M.I. Morsy, Role of surfactants in nanotechnology and their applications, Int. J. Curr. Microbiol. App. Sci. 3 (5) (2014) 237–260.
[5] L.Ya. Zakharova, A.B. Mirgorodskaya, E.P. Zhiltsova, L.A. Kudryavtseva, A.I. Konovalov, Reactions in supramolecular systems, in: U.H. Brinker, J.-L. Mieusset (Eds.), Molecular Encapsulation: Organic Reactions in Constrained Systems, John Willey and Sons, Chichester, U.K 2010, pp. 397–420.
[6] B.H. Lipshutz, S. Ghorai, M. Cortes-Clerget, The hydrophobic effect applied to organic synthesis: recent synthetic chemistry "in water", Chem. Eur. J. 24 (26) (2018) 6672–6695, https://doi.org/10.1002/chem.201705499.
[7] G. La Sorella, G. Strukul, A. Scarso, Recent advances in catalysis in micellar media, Green Chem. 17 (2015) 644–685, https://doi.org/10.1039/C4GC01368A.
[8] M.A. Malik, M.A. Hashim, F. Nabi, Sh.A AL-Thabaiti, Z. Khan, Anti-corrosion ability of surfactants: a review, Int. J. Electrochem. Sci. 6 (2011) 1927–1948.
[9] Y. Zhu, M.L. Free, R. Woollam, W. Durnie, A review of surfactants as corrosion inhibitors and associated modeling, Prog. Mater. Sci. 90 (2017) 159–223, https://doi.org/10.1016/j.pmatsci.2017.07.006 (DOI: 10.1016/j.pmatsci.2017.07.006).
[10] F. Devínsky, M. Pisárčik, M. Lukáč, Cationic Amphiphiles: Self-assembling Systems for Biomedicine and Biopharmacy, Nova Science Publishers, Inc, 2017.
[11] A.M. Grumezescu, Organic Materials as Smart Nanocarriers for Drug Delivery, 1st ed. William Andrew Publishing, Norwich, 2018.
[12] S. Ezrahi, A. Aserin, N. Garti, Basic principles of drug delivery systems – the case of paclitaxel, Adv. Colloid Interf. Sci. 263 (2019) 95–130, https://doi.org/10.1016/j.cis.2018.11.004.
[13] S.A. Rizvi, L. Shi, D. Lundberg, F.M. Menger, Unusual aqueous-phase behavior of cationic amphiphiles with hydrogen-bonding headgroups, Langmuir 24 (3) (2008) 673–677, https://doi.org/10.1021/la7037608.
[14] M.S. Borse, S. Devi, Importance of head group polarity in controlling aggregation properties of cationic gemini surfactants, Adv. Colloid Interf. Sci. 123–126 (2006) 387–399.
[15] L.Ya. Zakharova, R.R. Kashapov, T.N. Pashirova, A.B. Mirgorodskaya, O.G. Sinyashin, Self-assembly strategy for the design of soft nanocontainers with controlled properties, Mend. Comm. 26 (2016) 457–468, https://doi.org/10.1016/j.mencom.2016.11.001.
[16] A.K. Ghosh, M. Brindisi, Organic carbamates in drug design and medicinal chemistry, J. Med.Chem. 58 (7) (2015) 2895–2940, https://doi.org/10.1021/jm501371s.
[17] M. Pohanka, Inhibitors of acetylcholinesterase and butyrylcholinesterase meet immunity, Int. J. Mol. Sci. 15 (2014) 9809–9825, https://doi.org/10.3390/ijms15069809.
[18] J. Wu, M. Pistolozzi, S. Liu, W. Tan, Design, synthesis and biological evaluation of novel carbamates as potential inhibitors of acetylcholinesterase and butyrylcholinesterase, Bioorg. Med. Chem. 28 (5) (2020), 115324 https://doi.org/10.1016/j.bmc.2020.115324.
[19] S.K. Tippabhotla, N.R. Thudi, R. Raghuvanshi, A.H. Khuroo, S. Gurule, S. Mishra, T. Monif, V.K. Lao, A bioequivalence study comparing two formulations of lopinavir/ritonavir capsules, Int. J. Clin. Pharmacol. Ther. 46 (2008) 204–210, https://doi.org/10.5414/cpp46204.
[20] X. Wang, H. Mu, H. Chai, D. Liao, Q. Yao, C. Chen, Human immunodeficiency virus protease inhibitor ritonavir inhibits cholesterol efflux from human macrophage-derived foam cells, Am. J. Pathol. 171 (2007) 304–314, https://doi.org/10.2353/ajpath.2007.060965.
[21] G. Indolfi, D. Serranti, M. Resti, Direct-acting antivirals for children and adolescents with chronic hepatitis C, Lancet Child Adolesc. Health 2 (4) (2018) 298–304, https://doi.org/10.1016/S2352-4642(18)30037-3.
[22] C. Sikavi, H.Ph. Chen, A.D. Lee, E.G. Saab, G. Choi, S. Saab, Hepatitis C and human immunodeficiency virus coinfection in the era of direct-acting antiviral agents: no longer a difficult-to-treat population, Hepatology 67 (2018) 847–857, https://doi.org/10.1002/hep.29642.
[23] V.Y. Goloborodko, M.V. Strelkov, A.A. Kalinin, V.A. Byvaltsev, Analysis of efficacy of using nondepolarizing muscle relaxant rocuronium bromide and selective antidote sugammadex while providing general anesthesia to patients with degenerative spinal canal stenosis of the cervical spine, New Armenian Medical J. 11 (2017) 70–75.
[24] A.B. Mirgorodskaya, R.A. Kushnazarova, S.S. Lukashenko, A.D. Voloshina, O.A. Lenina, L.Ya. Zakharova, O.G. Sinyashin, Carbamate-bearing surfactants: Micellization, solubilization, and biological activity, J. Mol. Liq. 269 (2018) 203–210, https://doi.org/10.1016/j.molliq.2018.08.007.
[25] A.B. Mirgorodskaya, S.S. Lukashenko, R.A. Kushnazarova, R.R. Kashapov, L.Ya. Zakharova, O.G. Sinyashin, Amphiphilic compounds bearing a carbamate fragment: synthesis, aggregation, and solubilizing effect, Russ. J. Org. Chem. 54 (7) (2018) 987–991, https://doi.org/10.1134/S1070428018070023.
[26] A.B. Mirgorodskaya, R.A. Kushnazarova, A.Yu. Shcherbakov, S.S. Lukashenko, N.A. Zhukova, V.A. Mamedov, L.Ya. Zakharova, O.G. Sinyashin, Mixed systems based on the cationic surfactant with a butyl carbamate fragment and nonionic surfactant tween 80: aggregation behavior and solubilization properties, Russ. Chem. Bull. 67 (11) (2018) 1992–1996, https://doi.org/10.1007/s11172-018-2319-9.
[27] A.B. Mirgorodskaya, R.A. Kushnazarova, S.S. Lukashenko, L.Ya. Zakharova, Self-assembly of mixed systems based on nonionic and carbamate-bearing cationic surfactants as a tool for fabrication of biocompatible nanocontainers, J. Mol. Liq. 292 (2019), 111407 https://doi.org/10.1016/j.molliq.2019.111407.

[28] D.A. Kuznetsova, D.R. Gabdrakhmanov, L.R. Ahtamyanova, S.S. Lukashenko, A.M. Kusova, Yu.F. Zuev, A.D. Voloshina, A.S. Sapunova, N.V. Kulik, D.M. Kuznetsov, L. Ya Zakharova, Novel self-assembling systems based on imidazolium amphiphiles with cleavable urethane fragment for construction of soft nanocontainers for biomedicine application, J. Mol. Liq. 298 (2020) 111961, https://doi.org/10.1016/j.molliq.2019.111961.
[29] M. Aratono, N. Onimaru, Y. Yoshikai, M. Shigehisa, I. Koga, K. Wongwailikhit, A. Ohta, T. Takiue, B. Lhoussaine, R. Strey, Y. Takata, M. Villeneuve, H. Matsubara, Spontaneous vesicle formation of single chain and double chain cationic surfactant mixture, J. Phys. Chem. B 111 (1) (2007) 107–115, https://doi.org/10.1021/jp0637328.
[30] T. Ghaed-Sharaf, D.-Sh. Yang, S. Baldelli, M.H. Ghatee, From micelles to vesicle and membrane structures of double-strand ionic liquids in water: molecular dynamics simulation, Langmuir 35 (7) (2019) 2780–2791, https://doi.org/10.1021/acs.langmuir.8b03773.
[31] F.R. Alves, M.E. Zaniquelli, W. Loh, E.M. Castanheira, M.E. Real Oliveira, E. Feitosa, Vesicle-micelle transition in aqueous mixtures of the cationic dioctadecyldimethylammonium and octadecyltrimethylammonium bromide surfactants, J. Colloid Interface Sci. 316 (1) (2007) 132–139, https://doi.org/10.1016/j.jcis.2007.08.027.
[32] S. Koirala, B. Roy, P. Guha, R. Bhattarai, M. Sapkota, P. Nahak, G. Karmakar, A.K. Mandal, A. Kumard, A.K. Panda, Effect of double tailed cationic surfactants on the physicochemical behavior of hybrid vesicles, RSC Adv. 6 (2016) 13786–13796, https://doi.org/10.1039/C5RA17774J.
[33] A. Pinazo, V. Petrizelli, M. Bustelo, R. Pons, M.P. Vinardell, M. Mitjans, A. Manresa, L. Perez, New cationic vesicles prepared with double chain surfactants from arginine: role of the hydrophobic group on the antimicrobial activity and cytotoxicity, Colloids Surf., B. 141 (2016) 19–27, https://doi.org/10.1016/j.colsurfb.2016.01.020.
[34] P. Sakdiset, A. Okada, H. Todo, K. Sugibayashi, Selection of phospholipids to design liposome preparations with high skin penetration-enhancing effects, J. Drug Delivery Sci. Technol. 44 (2018) 58–64, https://doi.org/10.1016/j.jddst.2017.11.021.
[35] A. Zumbuehl, Artificial phospholipids and their vesicles, Langmuir 35 (32) (2019) 10223–10232, https://doi.org/10.1021/acs.langmuir.8b02601.
[36] J.N. Israelachvili, Intermolecular and Surface Forces, 3rd ed. Academic Press, 2011.
[37] J.R. Lakowicz, Principles of Fluorescence Spectroscopy, third ed. Springer, New York, 2006.
[38] A. Voloshina, V. Semenov, A. Strobykina, N. Kulik, E. Krylova, V. Zobov, V. Reznik, Synthesis and antimicrobial and toxic properties of novel 1,3-bis(alkyl)-6-methyluracil derivatives containing 1,2,3- and 1,2,4-triazolium fragments, Russ. J. Bioorg. Chem. 43 (2017) 170–176, https://doi.org/10.1134/S1068162017020170.
[39] T.N. Pashirova, E.M. Gibadullina, A.R. Burilov, R.R. Kashapov, E.P. Zhiltsova, V.V. Syakaev, W.D. Habicher, M.H. Rümmeli, Sh.K. Latypov, A.I. Konovalov, L.Ya. Zakharova, Amphiphilic O-functionalized calix[4]resocinarenes with tunable structural behavior, RSC Adv. 4 (20) (2014) 9912–9919, https://doi.org/10.1039/C3RA46146G.
[40] T.N. Pashirova, I.V. Zueva, K.A. Petrov, S.S. Lukashenko, I.R. Nizameev, N.V. Kulik, A.D. Voloshina, L. Almasy, M.K. Kadirov, P. Masson, E.B. Souto, L.Y. Zakharova, O.G. Sinyashin, Mixed cationic liposomes for brain delivery of drugs by the intranasal route: the acetylcholinesterase reactivator 2-PAM as encapsulated drug model, Colloids. Surf. B. 171 (2018) 358–367, https://doi.org/10.1016/j.colsurfb.2018.07.049.
[41] R. Ghosh, J. Dey, Vesicle formation by L -cysteine-derived unconventional single-tailed amphiphiles in water: a fluorescence, microscopy, and calorimetric investigation; spontaneous formation of a vesicular assembly by a trimesic acid based triple tailed amphiphile, Langmuir 30 (45) (2014) 13516–13524, https://doi.org/10.1021/la5022214.
[42] L. Piñeiro, M. Novo, W. Al-Soufi, Fluorescence emission of pyrene in surfactant solutions, Adv. Colloid Interf. Sci. 215 (2015) 1–12, https://doi.org/10.1016/j.cis.2014.10.010.
[43] N. Scholz, T. Behnke, U. Resch-Genger, Determination of the critical micelle concentration of neutral and ionic surfactants with fluorometry, conductometry, and surface tension–a method comparison, J. Fluoresc. 28 (2018) 465–476, https://doi.org/10.1007/s10895-018-2209-4.
[44] I.N. Kurniasih, H. Liang, P.Ch. Mohr, G. Khot, J.P. Rabe, A. Mohr, Nile red dye in aqueous surfactant and micellar solution, Langmuir 31 (9) (2015) 2639–2648, https://doi.org/10.1021/la504378m.
[45] N. Sarkar, K. Das, D.N. Nath, K. Bhattacharyya, Twisted charge transfer process of Nile Red in homogeneous solution and in faujasite zeolite, Langmuir 10 (1994) 326–329, https://doi.org/10.1021/la00013a048.
[46] M. Sutter, S. Oliveira, N.N. Sanders, B. Lucas, A. van Hoek, M.A. Hink, A.J. Visser, S.C. De Smedt, W.E. Hennink, W. Jiskoot, Sensitive spectroscopic detection of large and denatured protein aggregates in solution by use of the fluorescent dye Nile Red, J. Fluoresc. 17 (2) (2007) 181–192, https://doi.org/10.1007/s10895-007-0156-6.
[47] A. Okamoto, K. Tainaka, Y. Fujiwara, Nile Red nucleoside: design of a solvatofluorochromic nucleoside as an indicator of micropolarity around DNA, J. Org. Chem. 71 (9) (2006) 3592–3598, https://doi.org/10.1021/jo060168o.
[48] C. Lin, J. Zhao, R. Jiang, Nile red probing for the micelle-to-vesicle transition of AOT in aqueous solution, Chem. Phys. Lett. 464 (2008) 77–78, https://doi.org/10.1016/j.cplett.2008.09.001.
[49] V. Martinez, M. Henary, Nile red and Nile blue: applications and syntheses of structural analogues, Chemistry 22 (39) (2016) 13764–13782, https://doi.org/10.1002/chem.201601570.
[50] A. Mohanty, J. Dey, Effect of the headgroup structure on the aggregation behavior and stability of self-assemblies of sodium n-[4- (n-dodecyloxy)benzoyl]-l-aminoacidates in water, Langmuir 23 (2007) 1033–1040, https://doi.org/10.1021/la0625143.
[51] D. Khatua, J. Dey, Fluorescence, circular dichroism, light scattering, and microscopic characterization of vesicles of sodium salts of three n-acyl peptides, J. Phys. Chem. B 111 (2007) 124–130, https://doi.org/10.1021/jp065225w.
[52] A.B. Mirgorodskaya, L. Ya Zakharova, E.I. Khairutdinova, S.S. Lukashenko, O.G. Sinyashin, Supramolecular systems based on gemini surfactants for enhancing solubility of spectral probes and drugs in aqueous solution, Colloids Surf. A Physicochem. Eng. Asp. 510 (2016) 33–42, https://doi.org/10.1016/j.colsurfa.2016.07.065.
[53] T.C. Machado, A.B. Gelain, J. Rosa, S.G. Cardoso, Th. Caon, Cocrystallization as a novel approach to enhance the transdermal administration of meloxicam, Eur. J. Pharm. Sci. 123 (2018) 184–190, https://doi.org/10.1016/j.ejps.2018.07.038.
[54] A. Nokhodchi, Y. Javadzadeh, M.R. Siahi-Shadbad, M. Barzegar-Jalali, The effect of type and concentration of vehicles on the dissolution rate of a poorly soluble drug (indomethacin) from liquisolid compacts, J. Pharm. Pharm. Sci 8 (2005) 18–25.
[55] P.R. Babu, C.V. Subrahmany, J. Thimmasetty, R. Manavalan, K. Valliappan, Extended Hansen's solubility approach: meloxicam in individual solvents, Pak. J. Pharm. Sci. 20 (4) (2007) 311–316.
[56] V.V. Dhawan, M.S. Nagarsenker, Catanionic systems in nanotherapeutics - biophysical aspects and novel trends in drug delivery applications, J. Control. Release 266 (2017) 331–345, https://doi.org/10.1016/j.jconrel.2017.09.040.
[57] L. Jena, E. McErlean, H. McCarthy, Delivery across the blood-brain barrier: nanomedicine for glioblastoma multiforme, Drug Deliv. and Transl. Res. 10 (2020) 304–318, https://doi.org/10.1007/s13346-019-00679-2.